Letter

Anomalous temperature dependence of phonon pumping by ferromagnetic resonance in Co/Pd multilayers with perpendicular anisotropy

W. K. Peria,[1,*] D.-L. Zhang,[2] Y. Fan,[2] J.-P. Wang,[2] and P. A. Crowell[1]

[1]*School of Physics and Astronomy, University of Minnesota, Minneapolis, Minnesota 55455, USA*

[2]*Department of Electrical and Computer Engineering, University of Minnesota, Minneapolis, Minnesota 55455, USA*

(Received 1 October 2021; revised 19 July 2022; accepted 1 August 2022; published 18 August 2022)

We demonstrate the pumping of phonons by ferromagnetic resonance in a series of $[Co(0.8\,nm)/Pd(1.5\,nm)]_n$ multilayers ($n = 6$, 11, 15, and 20) with strong magnon-phonon coupling and perpendicular magnetic anisotropy. The effect is shown using broadband ferromagnetic resonance over a range of temperatures (10–300 K), where a resonant damping enhancement is observed at frequencies where the phonons can form standing waves across the multilayer. The strength of this effect is enhanced by approximately a factor of 4 at 10 K compared to room temperature, which is anomalous in the sense that the temperature dependence of the magnon-phonon coupling predicts an enhancement that is less than a factor of 2. We conclude by explaining how the stronger-than-expected temperature dependence highlights the essential role of dynamic magnetization pinning in driving the phonons.

DOI: 10.1103/PhysRevB.106.L060405

The ability to couple the spin degree of freedom with other degrees of freedom, such as charge or strain, is crucial to many spintronic applications. The coupling of spin to strain is a phenomenon known as magnetostriction, which is known to directly influence magnetization dynamics [1–10]. Some work on dynamical magnon-phonon coupling has focused on the generation of phonons by ferromagnetic resonance (FMR) in a magnetic thin film and subsequent propagation of the phonons into the substrate, which is referred to as phonon pumping [2,11–14]. Much of the early work on phonon pumping lacked broadband frequency dependence, which is necessary for fully characterizing the effect as well as demonstrating the existence of multiple resonances. Recent experimental work on phonon pumping has largely relied on time-resolved Kerr measurements [4,5,9], which are susceptible to strain excitation through laser heating rather than due to magnetization dynamics alone. Also, the temperature dependence of this effect has not been studied, which may provide new insights into the underlying physics.

In this Letter, we demonstrate the phonon pumping effect by ferromagnetic resonance in a series of $[Co/Pd]_n$ multilayers with perpendicular magnetic anisotropy (PMA). It is shown that the strength of the effect is strongly temperature dependent (a factor of ∼4 enhancement at 10 K relative to 300 K), much more than would be expected from the temperature dependence of the magnon-phonon coupling alone (less than a factor of 2 enhancement), which is due to the sensitivity of the phonon pumping to the pinning of the dynamic magnetization. We also show that the frequencies of the phonon pumping resonances can be tuned by varying n, the number of Co/Pd repetitions.

Co/Pd multilayers are well known for their strong magnon-phonon coupling and PMA [15] and have been demonstrated for use in perpendicular magnetic tunnel junctions (p-MTJ) [16], including cases where synthetic antiferromagnets (SAF) made from Co/Pd multilayers were used for the reference layers [17,18]. The PMA is particularly significant for this application since phonon pumping is more efficient for perpendicular magnetization. The reason is that the strongest coupling in this configuration is to transverse phonons propagating perpendicular to the interfaces [11,19,20], which can easily escape into the substrate. $[Co(0.8\,nm)/Pd(1.5\,nm)]_n$ multilayers ($n = 6$, 11, 15, and 20) were grown by dc magnetron sputtering at room temperature with a base pressure of $<5 \times 10^{-8}$ Torr using Ar gas at a working pressure of 2.0 mTorr. The thicknesses of the Co and Pd layers are 0.8 nm and 1.5 nm, respectively, for all of the samples and will henceforth be omitted. Ferromagnetic resonance (FMR) of the $[Co/Pd]_n$ multilayers [Fig. 1(a)] was measured using a coplanar waveguide setup with modulation of the applied magnetic field for lock-in detection of the transmitted microwave power, which was rectified with a Schottky diode detector. Further details of the experiment including example FMR line shapes are given in the Supplemental Material [21]. Magnetometry measurements were performed on all the multilayers using superconducting quantum interference device (SQUID) magnetometry. SQUID was used to measure hysteresis loops over a range of temperatures (5–300 K) for both in-plane and out-of-plane applied fields, which confirmed an out-of-plane easy axis in all the samples. SQUID was also used to measure the saturation magnetization as a function of temperature in the multilayers [21].

We first demonstrate the effect of phonon pumping on the FMR linewidths and how it depends on the number of Co/Pd repetitions in the multilayer stack. Figure 1(b) shows a schematic of the phonon pumping process, where magnetization dynamics are damped by the leakage of magnetoelastically driven phonons into the substrate. Figure 2 shows FMR linewidths measured in a perpendicular field as a function of frequency at 150 K for four different $[Co/Pd]_n$

*Corresponding author: peria@lanl.gov

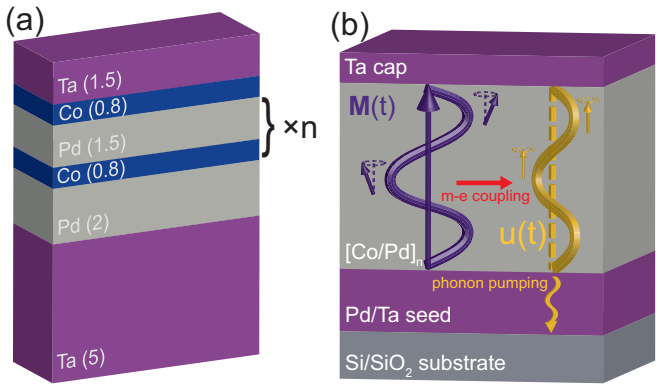

FIG. 1. (a) Stack structure of the $[Co/Pd]_n$ multilayers. Thicknesses of each layer are given in parentheses and have units of nm. The Co(0.8 nm)/Pd(1.5 nm) bilayer is repeated a total of n times as indicated on the figure. (b) Schematic of the phonon pumping process in the configuration where the magnetization $\mathbf{M}(t)$ is normal to the plane of the film. The magnetization depth profile is given by a sine wave (for simplicity) with pinning at the interfaces. The magnetoelastic coupling (shown by the red arrow) leads to the creation of a phonon standing wave with displacement $u(t)$. The phonon pumping process is shown by the wavy gold arrow representing the leakage of phonons into the seed layers and substrate.

multilayer structures with $n = 6$, 11, 15, and 20. The lower-frequency limit of the measurements is determined by the perpendicular anisotropy field (which sets the zero-field FMR frequency) for the $n = 6$ and 11 samples. For the $n = 15$ and 20 samples, the FMR signal disappears at nonzero field, which suggests that the sample becomes unsaturated at fields higher than zero. This observation is corroborated by

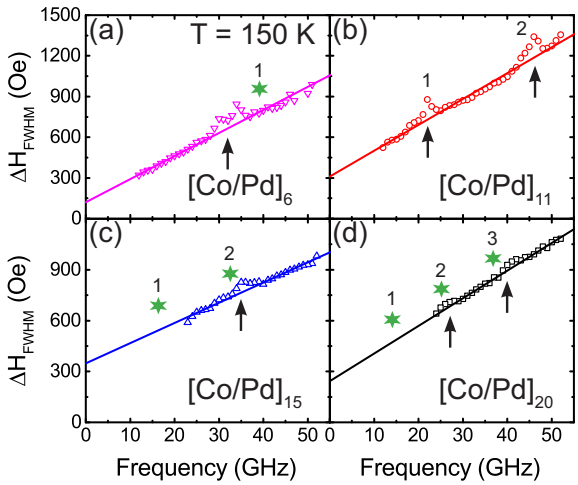

FIG. 2. Ferromagnetic resonance linewidths as a function of frequency with applied magnetic field out of plane at $T = 150$ K for (a) $[Co/Pd]_6$ (magenta triangles), (b) $[Co/Pd]_{11}$ (red circles), (c) $[Co/Pd]_{15}$ (blue triangles), and (d) $[Co/Pd]_{20}$ (black squares). The vertical arrows indicate the positions of the phonon pumping resonances, and the green stars indicate the corresponding positions predicted from the positions observed in the $[Co/Pd]_{11}$ multilayer. The numbers labeling the stars correspond to the number of half-waves in the thickness resonance so that, e.g., "3" means a phonon standing wave with wavelength $\lambda = 3d/2$, where d is the thickness of the magnetic portion of the multilayer.

out-of-plane magnetic hysteresis loops, which show the nucleation of domains before zero field is reached [21].

For all of the samples shown in Fig. 2, there are resonant linewidth enhancements that appear at specific frequencies. The linear background is due to the Gilbert damping, for which fits were generated by excluding points within 3 GHz of the center of the peaks. For the $n = 11$ and 20 multilayers, there are two resonant peaks in the linewidth. In the $n = 11$ multilayer, the frequency of the high-frequency peak is double that of the low-frequency peak, implying that these represent the first and second harmonics of a fundamental resonance. In the $n = 20$ multilayer, the high-frequency peak is 3/2 that of the low-frequency peak, suggesting that the low- and high-frequency peaks are the second and third harmonics of a fundamental resonance, respectively. We cannot observe the fundamental resonance, however, since it is expected at a frequency ($\simeq$ 13–14 GHz) at which the sample is unsaturated. For the $n = 6$ and 15 multilayers, there is one peak in the linewidth. This corresponds to the fundamental resonance in the $n = 6$ multilayer, and the second harmonic in the $n = 15$ multilayer. The fundamental resonance is undetectable in the $n = 15$ multilayer because it occurs at a frequency ($\simeq$ 16 GHz) at which the sample is unsaturated. We note that the resonance in the $[Co/Pd]_6$ multilayer exhibits a twin-peak structure, with the two peaks separated by approximately 4 GHz. This may be due to the existence of standing waves with nodes at both the interface between the 2-nm Pd and 5-nm Ta seed layers and the interface between the Co and 2-nm Pd seed layer [shown in Fig. 1(a)]. Were this the case, one would expect a spacing of about 4 GHz as we observe. This hypothesis predicts a peak spacing of $\lesssim 1$ GHz for the thicker multilayers, which would explain why the twin-peak structure is only observed in the $[Co/Pd]_6$ multilayer. We also observe a shift in the FMR field (dispersive response) coinciding with the resonances (absorptive response), which can be predicted accurately using Kramers-Kronig relations. This is shown in the Supplemental Material [21] for the $[Co/Pd]_6$ and $[Co/Pd]_{11}$ multilayers. Furthermore, the twin-peak structure observed in the linewidths for the $[Co/Pd]_6$ multilayer appears as a kink in the field shifts due to the antisymmetry of the dispersive response.

The vertical arrows in Fig. 2 indicate the positions of the resonances for each multilayer. Transverse acoustic phonon standing waves are expected at frequencies where d, the thickness of the stack excluding capping and seed layers, matches an integer number of phonon half wavelengths. This condition can be expressed as $f = c_t/(2d/m)$ (c_t is the transverse speed of sound and m is a positive integer). Longitudinal phonons are neglected because they couple to the magnetization at higher order [11,19,22]. The hypothesis that the multilayer is a half-wave resonator is based on the fact that the highly dense Ta capping and seed layers will lead to pinning of the phonons at these interfaces. The green stars in Figs. 2(a), 2(c) and 2(d) indicate the positions of the resonances predicted from the positions observed in the $[Co/Pd]_{11}$ multilayer in Fig. 2(b), where the effect is strongest. The numbers labeling the stars indicate the order of the resonance, so that a resonance of order m corresponds to a phonon standing wave of wavelength $\lambda = 2d/m$. From this we note that there is good agreement between the observed and predicted positions of the resonances,

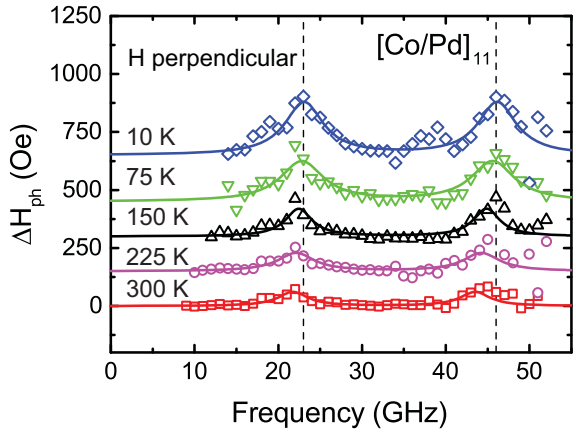

FIG. 3. Evolution of the phonon pumping contribution to the FMR linewidths ΔH_{ph} with temperature for the $[Co/Pd]_{11}$ multilayer at temperatures of 10 K (blue diamonds), 75 K (green triangles), 150 K (black triangles), 225 K (magenta circles), and 300 K (red squares). The applied magnetic field is perpendicular to the multilayer plane. The vertical dashed lines indicate the locations of the phonon pumping peaks, 23 GHz and 46 GHz (at 10 K), which correspond to phonon wavelengths of $\lambda = 2d$ and $\lambda = d$, respectively, where d is the thickness of the multilayer (excluding capping and seed layers). The data below 300 K are offset vertically so that the individual data sets could be more easily distinguished.

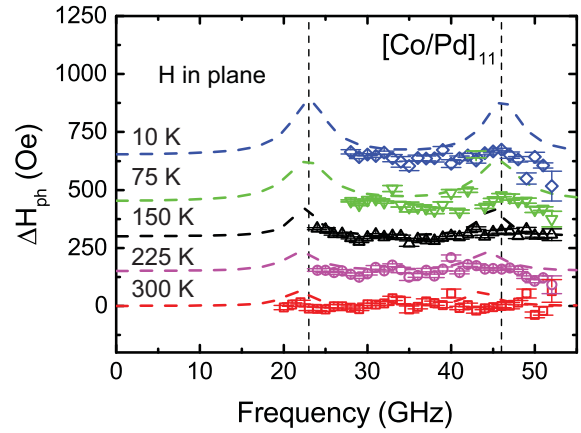

FIG. 4. Ferromagnetic resonance linewidths, with Gilbert damping and inhomogeneous broadening contributions subtracted, as a function of frequency for the $[Co/Pd]_{11}$ multilayer at temperatures of 10 K (blue diamonds), 75 K (green triangles), 150 K (black triangles), 225 K (magenta circles), and 300 K (red squares). The applied magnetic field is in the plane of the multilayer. The dashed curves are the fits for perpendicular fields shown in Fig. 3, plotted for the purposes of contrast. The data below 300 K were given a positive vertical offset so that the individual data sets could be more easily distinguished.

which demonstrates that the resonances can indeed be thought of as thickness resonances. The most significant deviation is observed in the $[Co/Pd]_6$ sample, which is the thinnest and therefore most sensitive to changes in the effective thickness at the top and bottom interfaces.

The temperature dependence of the phonon pumping contribution to the FMR linewidths of the $[Co/Pd]_{11}$ multilayer is shown in Fig. 3 for temperatures ranging from 10–300 K. The phonon pumping contribution is quantified by fitting the full width at half-maximum (FWHM) FMR linewidths to the form

$$\Delta H_{\mathrm{FWHM}} = \Delta H_0 + 2\alpha\omega/\gamma + \Delta H_{ph}(\omega)\,, \qquad (1)$$

where ΔH_0 is the frequency-independent inhomogeneous broadening, $2\alpha\omega/\gamma$ is the contribution from Gilbert damping (α is the Gilbert damping constant and γ is the gyromagnetic ratio), and $\Delta H_{ph}(\omega)$ is the nonlinear frequency-dependent contribution from phonon pumping. We assume a phenomenological Lorentzian line shape for the form of $\Delta H_{ph}(\omega)$:

$$\Delta H_{ph}(\omega) = \sum_n 2A_n \frac{\delta\omega/2}{(\omega - n\omega_0)^2 + (\delta\omega/2)^2}\,, \qquad (2)$$

where $\delta\omega$ is the FWHM of the resonance, ω_0 is the frequency of the fundamental half-wave resonance, and A_n sets the amplitude (the factor of 2 is needed to convert from HWHM to FWHM). In the case of the $[Co/Pd]_{11}$ multilayer, we enforce the constraints that the high-frequency resonance is exactly twice the low-frequency resonance and that the amplitudes of both resonances are equal. The widths of the resonances—inversely proportional to the lifetime of the phonons in the multilayer—are set by the acoustic impedance ratios at the boundaries, so that a strong mismatch will yield a sharp resonance [2,3,11,20,23]. In principle, phonon relaxation within the multilayer can influence the resonance width [3,20,23], but this is likely negligible since the widths are independent of temperature; the elastic coupling of the multilayer to the substrate, which determines the width of the resonances for the case of phonon pumping, depends negligibly on temperature, which is not generally the case for phonon relaxation in the multilayer [10,24].

It is clear from Fig. 3 that the intensity of the thickness resonances increases strongly at low temperature (whereas the Gilbert damping depends very weakly on temperature, as shown in the Supplemental Material [21]). The amplitudes of the resonances are about a factor of 4 larger at 10 K relative to 300 K. A strong temperature dependence of the amplitude of the resonances is seen for all of the multilayers, increasing at low temperature by a magnitude similar to that seen in Fig. 3 for the $[Co/Pd]_{11}$ sample. Also noteworthy is the small upward shift in the frequency of the resonances with decreasing temperature. This is consistent with the expectation that the elastic moduli should increase at low temperature, causing an increase in the speed of sound (which is proportional to the frequency of a given thickness resonance). The frequencies of the first and second thickness resonances shift from 22 and 44 GHz to 23 and 46 GHz, respectively. We did not observe any thickness resonances for in-plane magnetization (shown in Fig. 4), which is expected due to the fact that the strongest coupling is to phonons propagating parallel to the static magnetization [11,19,22]. The dashed curves in Fig. 4 are identical to the solid curves in Fig. 3, making it clear that the thicknesses resonances are absent for the in-plane case.

There has been significant theoretical work attempting to model phonon pumping [11,13,20,22,23,25–27], and so we will not give a comprehensive overview here. All models

predict that the phonon pumping amplitude should go as the square of the magnetoelastic coefficient, which can be understood in terms of Fermi's golden rule. One of the primary factors influencing the phonon pumping is the nonuniformity of the dynamic magnetization, which is necessary for exciting acoustic phonons (since they have nonzero wave vector). The model presented by Streib *et al.* [11] assumes uniform magnetization within the film, with the only nonuniformity coming from the discontinuity of the magnetization at the interfaces of the film. It is important to note that this model predicts the excitation of only odd-integer half-wave resonances ($d = \lambda/2, 3\lambda/2, ...$) due to destructive interference at frequencies where the phonons are even-integer half-waves. Our data show clearly that both even and odd resonances are excited, however, which relates to the fact that the dynamic magnetization in these multilayers is certainly nonuniform. Furthermore, the boundary conditions likely differ at the bounding interfaces at the top and bottom of the multilayer (Ta/Co on top and Co/Pd on bottom). The interior of the multilayer also promotes nonuniform static magnetization due to the nonuniformity inherent in the proximity-induced magnetism in the Pd layers. The differences between our observations and the predictions of the model of Streib *et al.* [11] underscore the importance of boundary conditions in the phonon pumping process, and it is probable that the complex magnetization depth profile associated with magnetic multilayers serves to enhance the phonon pumping.

The temperature dependence of the phonon pumping strength is expected to be primarily due to the dependence of magnetostriction on temperature [2,11]. It can be shown that since the magnetoelastic energy is quadratic in the magnetization cosines [19], the magnetoelastic energy should scale with temperature as $m^3(T)$ [28–30], where $m(T) \equiv M(T)/M(0)$ is the reduced magnetization. As mentioned earlier, the phonon pumping amplitude depends on the square of the magnetoelastic energy and would therefore be expected to scale with temperature as m^6.

Figure 5 shows the temperature dependence of the maximum value of $\Delta H_{ph}(\omega)$ for all the multilayers, normalized by the maximum value at 10 K. The damping enhancement depends quite strongly on temperature, with the effect being a factor of at least 4 greater at low temperature compared to room temperature. This depends on temperature much more strongly than m^6 (shown in the insets of Fig. 5), which ranges from $\simeq$ 0.65–0.75 at 300 K in the four multilayers. In addition to the magnetoelastic coupling, the pinning of the dynamic magnetization can strengthen the coupling to phonons since they are driven by variations in the magnetization [19]. The pinning at the exterior interfaces of the multilayer [Co/Ta on the top and Co/Pd on the bottom, see Fig. 1(a)] becomes stronger at low temperature due to an increase in the interfacial anisotropy energy [30]. The pinning is also seen to have an effect on the FMR field, observed through a stronger-than-expected temperature dependence of the interface anisotropy measured with FMR [21]. The estimated magnitude of the pinning field (∼1 kOe) [21] is about a factor of 10 smaller than the interface anisotropy field (∼10 kOe), so the pinning produces an effect of reasonable magnitude.

The Co/Pd multilayer system is an ideal platform for phonon pumping due to the strong magnon-phonon interaction and PMA, which opens up the possibility of engineering devices that utilize this effect at zero applied field in the advantageous perpendicular configuration. As we have demonstrated, the frequency of the phonon pumping resonance is highly tunable through the number of Co/Pd repetitions, which notably does not significantly affect the magnitude of the PMA. It is therefore feasible to engineer a Co/Pd multilayer that experiences a phonon pumping resonance at zero external field.

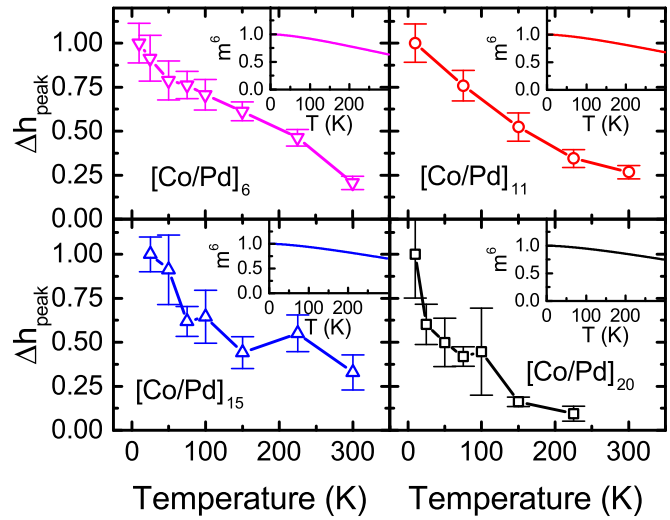

FIG. 5. Normalized peak values of $\Delta H_{ph}(\omega)$ as a function of temperature, defined by $\Delta h_{\text{peak}} \equiv \Delta H_{\text{peak}}(T)/\Delta H_{\text{peak}}(10\text{ K})$, for the (a) $[\text{Co/Pd}]_6$, (b) $[\text{Co/Pd}]_{11}$, (c) $[\text{Co/Pd}]_{15}$, and (d) $[\text{Co/Pd}]_{20}$ multilayers. Insets show m^6 as a function of temperature.

In conclusion, we report a strong phonon pumping effect in a series of Co/Pd PMA multilayers. The phonon pumping is observed primarily through resonant damping enhancements of the FMR mode, which are determined by the thickness of the multilayer. The phonon pumping effect is strongly enhanced at low temperatures, stronger than would be expected from the temperature dependence of the magnon-phonon coupling alone. The pinning of the dynamic magnetization serves to enhance the coupling between the two modes, and is ultimately responsible for the anomalous temperature dependence since the pinning becomes stronger at low temperature. Our results indicate that interfacial engineering will play a key role in either enhancing or suppressing this process, and should be an emphasis of future work.

This work was supported by SMART, a center funded by nCORE, a Semiconductor Research Corporation program sponsored by NIST. Parts of this work were carried out in the Characterization Facility, University of Minnesota, which receives partial support from NSF through the MRSEC program, the Minnesota Nano Center, which is supported by NSF through the National Nano Coordinated Infrastructure Network, Award No. NNCI - 1542202, and the Institute for Rock Magnetism (IRM) at the University of Minnesota, a U.S. National Multi-user Facility supported through the Instrumentation and Facilities program of the National Science Foundation, Earth Sciences Division, under Award No. NSF EAR-1642268 and by funding from the University of Minnesota.

[1] H. Bömmel and K. Dransfeld, Excitation of Hypersonic Waves by Ferromagnetic Resonance, Phys. Rev. Lett. **3**, 83 (1959).

[2] M. Seavey, Phonon generation by magnetic films, Proc. IEEE **53**, 1387 (1965).

[3] R. Weber, Magnon-phonon coupling in metallic films, Phys. Rev. **169**, 451 (1968).

[4] J. V. Jäger, A. V. Scherbakov, T. L. Linnik, D. R. Yakovlev, M. Wang, P. Wadley, V. Holy, S. A. Cavill, A. V. Akimov, A. W. Rushforth, and M. Bayer, Picosecond inverse magnetostriction in galfenol thin films, Appl. Phys. Lett. **103**, 032409 (2013).

[5] J. V. Jäger, A. V. Scherbakov, B. A. Glavin, A. S. Salasyuk, R. P. Campion, A. W. Rushforth, D. R. Yakovlev, A. V. Akimov, and M. Bayer, Resonant driving of magnetization precession in a ferromagnetic layer by coherent monochromatic phonons, Phys. Rev. B **92**, 020404(R) (2015).

[6] J. Holanda, D. S. Maior, A. Azevedo, and S. M. Rezende, Detecting the phonon spin in magnon–phonon conversion experiments, Nature Phys. **14**, 500 (2018).

[7] K. An, A. N. Litvinenko, R. Kohno, A. A. Fuad, V. V. Naletov, L. Vila, U. Ebels, G. de Loubens, H. Hurdequint, N. Beaulieu, J. Ben Youssef, N. Vukadinovic, G. E. W. Bauer, A. N. Slavin, V. S. Tiberkevich, and O. Klein, Coherent long-range transfer of angular momentum between magnon Kittel modes by phonons, Phys. Rev. B **101**, 060407(R) (2020).

[8] C. Zhao, Y. Li, Z. Zhang, M. Vogel, J. E. Pearson, J. Wang, W. Zhang, V. Novosad, Q. Liu, and A. Hoffmann, Phonon Transport Controlled by Ferromagnetic Resonance, Phys. Rev. Appl. **13**, 054032 (2020).

[9] D.-L. Zhang, J. Zhu, T. Qu, D. M. Lattery, R. H. Victora, X. Wang, and J.-P. Wang, High-frequency magnetoacoustic resonance through strain-spin coupling in perpendicular magnetic multilayers, Sci. Adv. **6**, eabb4607 (2020).

[10] W. K. Peria, X. Wang, H. Yu, S. Lee, I. Takeuchi, and P. A. Crowell, Magnetoelastic Gilbert damping in magnetostrictive $Fe_{0.7}Ga_{0.3}$ thin films, Phys. Rev. B **103**, L220403 (2021).

[11] S. Streib, H. Keshtgar, and G. E. W. Bauer, Damping of Magnetization Dynamics by Phonon Pumping, Phys. Rev. Lett. **121**, 027202 (2018).

[12] A. Rückriegel and R. A. Duine, Long-Range Phonon Spin Transport in Ferromagnet–Nonmagnetic Insulator Heterostructures, Phys. Rev. Lett. **124**, 117201 (2020).

[13] X. Zhang, G. E. W. Bauer, and T. Yu, Unidirectional Pumping of Phonons by Magnetization Dynamics, Phys. Rev. Lett. **125**, 077203 (2020).

[14] S. M. Rezende, D. S. Maior, O. Alves Santos, and J. Holanda, Theory for phonon pumping by magnonic spin currents, Phys. Rev. B **103**, 144430 (2021).

[15] S. Hashimoto, Y. Ochiai, and K. Aso, Perpendicular magnetic anisotropy and magnetostriction of sputtered Co/Pd and Co/Pt multilayered films, J. Appl. Phys. **66**, 4909 (1989).

[16] Z. R. Tadisina, A. Natarajarathinam, B. D. Clark, A. L. Highsmith, T. Mewes, S. Gupta, E. Chen, and S. Wang, Perpendicular magnetic tunnel junctions using Co-based multilayers, J. Appl. Phys. **107**, 09C703 (2010).

[17] A. Natarajarathinam, R. Zhu, P. B. Visscher, and S. Gupta, Perpendicular magnetic tunnel junctions based on thin CoFeB free layer and Co-based multilayer synthetic antiferromagnet pinned layers, J. Appl. Phys. **111**, 07C918 (2012).

[18] Y.-J. Chang, A. Canizo-Cabrera, V. Garcia-Vazquez, Y.-H. Chang, and T.-h. Wu, Perpendicular magnetic tunnel junctions with synthetic antiferromagnetic pinned layers based on [Co/Pd] multilayers, J. Appl. Phys. **113**, 17B909 (2013).

[19] C. Kittel, Interaction of spin waves and ultrasonic waves in ferromagnetic crystals, Phys. Rev. **110**, 836 (1958).

[20] R. L. Comstock and R. C. LeCraw, Generation of microwave elastic vibrations in a disk by ferromagnetic resonance, J. Appl. Phys. **34**, 3022 (1963).

[21] See Supplemental Material at http://link.aps.org/supplemental/10.1103/PhysRevB.106.L060405. for details of the FMR experiment, temperature dependence of magnetic moment and interface anisotropy, and a discussion of the effect of phonon pumping on the FMR field.

[22] T. Sato, W. Yu, S. Streib, and G. E. W. Bauer, Dynamic magnetoelastic boundary conditions and the pumping of phonons, Phys. Rev. B **104**, 014403 (2021).

[23] M. H. Seavey, Boundary-value problem for magnetoelastic waves in a metallic film, Phys. Rev. **170**, 560 (1968).

[24] A. I. Bezuglyj, V. A. Shklovskij, V. V. Kruglyak, and R. V. Vovk, Temperature dependence of the magnon-phonon energy relaxation time in a ferromagnetic insulator, Phys. Rev. B **100**, 214409 (2019).

[25] M. Seavey, Microwave phonon generation by thin magnetic films, IEEE Trans. Ultrason. Eng. **10**, 49 (1963).

[26] C. F. Kooi, Interaction of phonons and spin waves, Phys. Rev. **131**, 1070 (1963).

[27] T. Kobayashi, R. C. Barker, J. L. Bleustein, and A. Yelon, Ferromagnetoelastic resonance in thin films. I. formal treatment, Phys. Rev. B **7**, 3273 (1973).

[28] C. Kittel and J. H. Van Vleck, Theory of the temperature dependence of the magnetoelastic constants of cubic crystals, Phys. Rev. **118**, 1231 (1960).

[29] E. R. Callen and H. B. Callen, Static magnetoelastic coupling in cubic crystals, Phys. Rev. **130**, 2600 (1963).

[30] H. Callen and E. Callen, The present status of the temperature dependence of magnetocrystalline anisotropy, and the $l(l+1)/2$ power law, J. Phys. Chem. Solids **27**, 1271 (1966).